

## Role of p-GaN layer thickness in the degradation of InGaN-GaN MQW solar cells under 405 nm laser excitation

Marco Nicoletto<sup>a,\*</sup>, Alessandro Caria<sup>a</sup>, Carlo De Santi<sup>a</sup>, Matteo Buffolo<sup>a</sup>, Xuanqi Huang<sup>b</sup>, Houqiang Fu<sup>c</sup>, Hong Chen<sup>b</sup>, Yuji Zhao<sup>b,d</sup>, Gaudenzio Meneghesso<sup>a</sup>, Enrico Zanoni<sup>a</sup>, Matteo Meneghini<sup>a</sup>

<sup>a</sup> Department of Information Engineering, University of Padova, via Gradenigo 6/B, Padova 35131, Italy

<sup>b</sup> School of Electrical, Computer, and Energy Engineering, Arizona State University, Tempe, AZ 85287, USA

<sup>c</sup> Department of Electrical and Computer Engineering, Iowa State University, Ames, IA 50011, USA

<sup>d</sup> Department of Electrical and Computer Engineering, Rice University, Houston, TX 77005, USA

### ARTICLE INFO

#### Keywords:

GaN  
InGaN  
p-GaN  
Multiple-Quantum-Wells  
Solar cells  
Degradation  
Reliability  
Temperature  
Constant optical power stress

### ABSTRACT

GaN-based solar cells with InGaN multiple quantum wells (MQWs) are promising devices for application in space environment, concentrator solar systems, wireless power transmission and multi-junction solar cells. It is therefore important to understand their degradation kinetics when submitted to high-temperature and high-intensity stress. We submitted three samples of GaN-InGaN MQW solar cells with p-AlGaIn electron-blocking-layer with different thickness of the p-GaN layer to constant power stress at 310 W/cm<sup>2</sup>, 175 °C for several hundred hours. The main degradation modes are a reduction of open-circuit voltage, short-circuit current, external quantum efficiency, power conversion efficiency and electroluminescence. In particular, we observed that a thinner p-GaN layer results in a stronger degradation observed on the cell operating parameters. The analysis of the dark I-V characteristics showed an increase in low-forward bias current and the analysis of electroluminescence showed a decrease in the electroluminescence emitted by the (forward biased) cell, as a consequence of stress. This work highlights that the cause of degradation is possibly related to a diffusion mechanism, which results in an increase of defect density in the active region. The impurities involved in the diffusion processes possibly originate from the p-side of the devices, therefore a thicker p-GaN layer reduces the amount of defects reaching the active region.

### 1. Introduction

Renewable and sustainable forms of energy are becoming more and more important, to support human growth and reduce global warming. For this reason, several new technologies have been developed in the last decades to increase solar energy conversion. In particular, record efficiencies (47 %) have been obtained for multi-junctions solar cells [1], and new materials are under study to further push the performance to higher levels. Among these, the GaN-InGaIn material system is subject of investigation, leveraging on the knowledge gained in the development of multi-quantum wells (MQW) structures for application in general lighting (LEDs, laser diodes). InGaIn-based photodetectors and solar cells have been proposed for concentrator solar harvesting systems [2,3], wireless power transfer [4] and space applications [5] also thanks to their reliability in harsh environments [6].

However, the degradation mechanisms of InGaIn solar cells and photodetectors are largely unexplored. For this reason, in this work, we studied the degradation of three samples of GaN-based MQW solar cells with different p-GaN layer thickness under high power monochromatic (405 nm) laser excitation, and under high baseplate temperature (175 °C). Results allow to understand the behavior of the cells in high temperature and high illumination conditions. In addition, we shed light on the cause of degradation, which is ascribed to the presence of diffusion mechanisms. Finally, we investigate the influence of the p-GaN layer thickness on these processes.

### 2. Experimental details

The devices under tests (Fig. 1) are GaN/InGaIn MQW solar cells grown on c-plane sapphire by metal-organic chemical vapor deposition

\* Corresponding author.

E-mail address: [marco.nicoletto.2@studenti.unipd.it](mailto:marco.nicoletto.2@studenti.unipd.it) (M. Nicoletto).

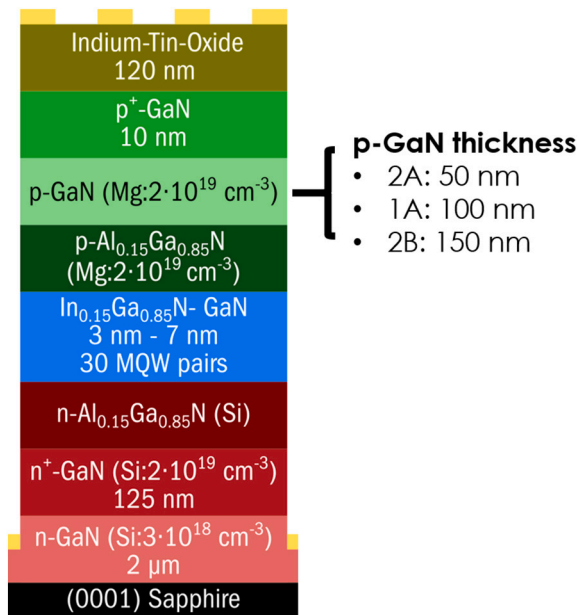


Fig. 1. Device structure. Difference in  $T_{p\text{-GaN}}$  length: 2A 50 nm, 1A 100 nm and 2B 150 nm.

(MOCVD). On (0001) sapphire substrate, a 2  $\mu\text{m}$  n-GaN (Si doped,  $3 \cdot 10^{18} \text{ cm}^{-3}$ ) layer and a 125 nm  $n^+$ -GaN (Si doped,  $2 \cdot 10^{19} \text{ cm}^{-3}$ ) layer are grown. Then, the active region consists in a periodic structure made by 30 pairs of undoped  $\text{In}_{0.15}\text{Ga}_{0.85}\text{N}$  quantum wells (3 nm) and GaN barriers (7 nm). Over the active region, a 5 nm  $p\text{-Al}_{0.15}\text{Ga}_{0.85}\text{N}$  electron blocking layer (Mg doped,  $2 \cdot 10^{19} \text{ cm}^{-3}$ ) is grown, followed by a p-GaN layer (Mg doped,  $2 \cdot 10^{19} \text{ cm}^{-3}$ ), a 10 nm  $p^+$ -GaN layer (Mg doped,  $> 2 \cdot 10^{19} \text{ cm}^{-3}$ ) and a semitransparent 120 nm indium-tin oxide (ITO) layer. The Mg activation rate is about 1 %, so a  $2 \cdot 10^{19}$  Mg doping level in the p-GaN layer leads to an estimated hole concentration around  $1 \cdot 10^{17} \text{ cm}^{-3}$ . The  $p^+$ -GaN layer is used to create a ohmic contact with metal, thus minimizing contact resistivity. Finally, devices are processed by standard lithography in  $1 \times 1 \text{ mm}^2$  solar cells. Ti/Al/Ni/Au ring contacts and Ti/Pt/Au grid contacts were deposited around the perimeter and on the top of the mesa to form cathode and anode contacts. Further details are available in Huang et al. [7]. The three samples analyzed in this paper differ only in the thickness  $T_{p\text{-GaN}}$  of the p-GaN layer: sample 2A has a p-GaN layer of 50 nm, sample 1A of 100 nm and sample 2B of 150 nm.

Samples were contacted by tungsten micro-tips and mounted on a thermal-controlled baseplate, heated by a ceramic heater. The optical excitation to stress the devices during the medium-term (100/500 h) constant optical power stress was provided by means of high power 405 nm laser diode (nominal output power  $> 2 \text{ W}$ ). The optical stress was performed with an optical density equal to  $310 \text{ W/cm}^2$  at  $175 \text{ }^\circ\text{C}$ , then, after each step of the stress, the devices are characterized at  $35 \text{ }^\circ\text{C}$  by means of dark and illuminated current-voltage (I-V) measurements (using the same laser diode for illuminated I-V), electroluminescence-current (L-I) measurements and photocurrent measurements. A Semiconductor Parameter Analyzer was used to obtain high accuracy measurements. During illuminated I-V a motorized filter wheel was used to insert several neutral density filters in the optical path to reduce the output power of the laser beam and to allow performing low intensity illuminated characterizations. Monochromatic light for photocurrent characterization was generated by a 300 W Xenon arc-lamp which output was delivered on the sample by a fiber and focusing system.

### 3. Experimental results and discussion

The constant optical power stress consists of a succession of steps of increasing time duration up to 100 h (for sample 2A) or 500 h (for sample 1A and 2B). These stress tests were carried out at baseplate temperature of  $175 \text{ }^\circ\text{C}$ . The overall duration of stress differs between the samples because, after 100 h of stress, only sample 2A showed a significant degradation, while for the other samples it was necessary to increase the stress time to observe a significant degradation (this can be seen by comparing the decrease in the normalized short-circuit current measured during the constant optical power stress after a total stress time of 6000 min in Fig. 2). In Table 1 are presented the different time steps of the stress.

Fig. 2 reports the normalized short-circuit current monitored during each step of the constant power stress at  $175 \text{ }^\circ\text{C}$ . The stress causes a decrease in the short-circuit current. The main outcome of the stress is that sample 2A ( $T_{p\text{-GaN}} = 50 \text{ nm}$ ) presents the highest decrease in short-circuit current after 100 h of stress, namely  $\sim 11 \%$  of relative decrease, while the other samples do not show any decrease after 100 h. Instead, after 500 h of stress, sample 1A ( $T_{p\text{-GaN}} = 100 \text{ nm}$ ) and 2B ( $T_{p\text{-GaN}} = 150 \text{ nm}$ ) show a relative decrease of  $\sim 3 \%$  and  $\sim 2 \%$  respectively. The analysis of the stress shows that the lower the thickness of the p-GaN layer, the higher the decrease in the short-circuit current during the stress.

The analysis of the dark I-V characteristics, with the current at 1.25 V (inset), shown in Fig. 3, shows that the sample with the thinner  $T_{p\text{-GaN}}$  has the strongest degradation of the I-V characteristics, confirming that the thickness of this layer is a key parameter in the degradation of these devices. In particular, the sample with the thinner p-GaN layer shows a significant increase in forward current at low bias levels (below the main diode turn-on voltage). This behavior can be ascribed to the presence of traps located in the active region, since it is well-known that trap-assisted forward tunneling gives the most relevant contribution to current flow below the optical turn-on of the main diode [8–10]. Considering the current at 1.25 V (insets of Fig. 3), samples 1A and 2B show no variation or a small decrease, while sample 2A has a significant increase: the current increases by two orders of magnitude with respect to the unstressed sample. This behavior can be fitted with a straight line with slope  $\sim 0.58$  (in log-log scale, which approximately corresponds to a square root dependence on time). In particular, this could indicate the presence of a thermally-activated diffusion process, since 1D diffusion process can be described as:

$$R(t, x) = R_0 \operatorname{erfc} \left( \frac{x}{2\sqrt{Dt}} \right) \quad (1)$$

where  $R(t, x)$  is the impurity concentration at time  $t$  and position  $x$ ,  $R_0 = R(t = 0)$  and  $D$  is the diffusion coefficient [9]. A study to better understand, characterize and model the process responsible for diffusion is in progress. However, hydrogen is a strong candidate as a diffusant involved in the degradation, as reported in other studies of different.

GaN/InGaN structures [9]. Contribution to material defectiveness and/or non-ideal material composition may originate from: 1) the well-known problems of Mg memory effect and Mg surface segregation [10]; 2) the presence of a thin, highly doped,  $p^+$ -GaN layer before the ITO layer, where different types of vacancies and defects could originate [11]; 3) the fact that large amounts of H atoms are incorporated into the p-type layers (doped with Magnesium with a Mg density of  $10^{18} \text{ cm}^{-3}$  to  $10^{19} \text{ cm}^{-3}$ ) during MOCVD growth; 4) the fact that the hydrogen density may remain high even after Mg activation [12]. Impurities coming from the top-side of the cell can diffuse towards the active region. Besides the mentioned contribution of H [13], the presence of gallium vacancies or oxygen may also favor the degradation kinetics ( $V_{\text{Ga}}$  can originate at the ITO/ $p^+$ -GaN interface [11], while oxygen [14] coming from ITO layer, can diffuse via threading dislocations in GaN [13]). Considering that the three samples only differ in the thickness of the p-GaN layer and that

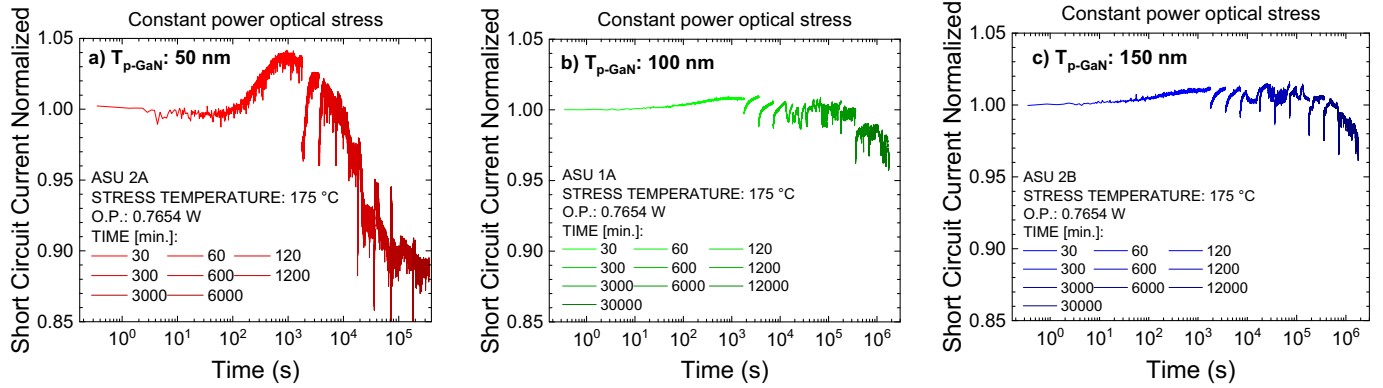


Fig. 2. Constant power optical stress. Comparison between short-circuit current monitored during the stress normalized to the first data of the first step for the three samples: a) 2A  $T_{p-GaN} = 50$  nm b) 1A  $T_{p-GaN} = 100$  nm c) 2B  $T_{p-GaN} = 150$  nm.

Table 1

Time step of the stress and total stress time at the end of each step.

Step number	Time step duration [minutes]	Total time stress duration [minutes]
1	30	30
2	30	60
3	60	120
4	180	300
5	300	600
6	600	1200
7	1800	3000
8	3000	6000
9 (only for 1A and 2B)	6000	12,000
10 (only for 1A and 2B)	18,000	30,000

diffusants involved in the thermal-activated diffusion process can mainly come from the ending layers of the device, thus ITO and  $p^+$ -GaN, a thicker p-GaN layer can reduce the amount of impurities which diffuse in the active region leading to a reduced degradation.

A similar behavior is shown by electroluminescence versus current graphs, plotted in Fig. 4. As can be noticed, a higher electroluminescence signal was detected in sample 2B ( $T_{p-GaN} = 150$  nm), possibly due to an active region with lower concentration of defects with respect to the other samples. Sample 2A ( $T_{p-GaN} = 50$  nm) does not emit below 1 mA, while the other samples emit in the same current range. Furthermore, sample 2A shows a strong decrease in luminescence during the stress (at the driving current of 0.01 A the optical power has a decrease of ~50 % compared to the unstressed sample), while sample 1A ( $T_{p-GaN} = 100$  nm) shows a lower degradation (decrease of ~5 % at 0.01 A with respect to

the unstressed sample) and sample 2B does not show degradation, as can be seen in the insets of Fig. 4. Even in this characterization, for sample 2A the optical power at 10 mA with respect to the stress time can be interpolated with a line having ~-0.2 slope (in log-log scale), that can be compatible with a thermally-activated diffusion process. This trend is less evident for the other samples with thicker p-GaN, suggesting another time that a larger p-GaN layer can reduce the amount of impurities which diffuses to the active region, leading to a smaller decrease in the EL signal, due to a lower amount of defects which can act as non-radiative recombination centers.

The trend of the open-circuit voltage with respect to the stress time at different intensities is shown in Fig. 5. In this figure the open-circuit voltage at different intensities is normalized with respect to the open-circuit voltage measured on the unstressed device. For sample 2A ( $T_{p-GaN} = 50$  nm), the open-circuit voltage presents a relative decrease of ~15 % at higher intensities while the other samples present an almost unchanged open-circuit voltage. This confirms the hypothesis of lower amount of defects in the active region, possibly due to a thermally-activated diffusion process, which reduces the charge in the active region leading to a reduction of the open-circuit voltage.

As discussed above, the thickness of the p-GaN layer, is a key parameter for the stability of solar cells, especially for concentrator solar harvesting systems [2,3] and in space applications [4]. It is worth noticing that the p-GaN layer thickness has also a crucial role in the quantum efficiency of these devices. P-GaN has a high absorption, and strongly impacts on the amount of light that can reach the junction, as demonstrated by our recent modeling investigations [15,16], so a trade-off between performance and long-term reliability has to be considered.

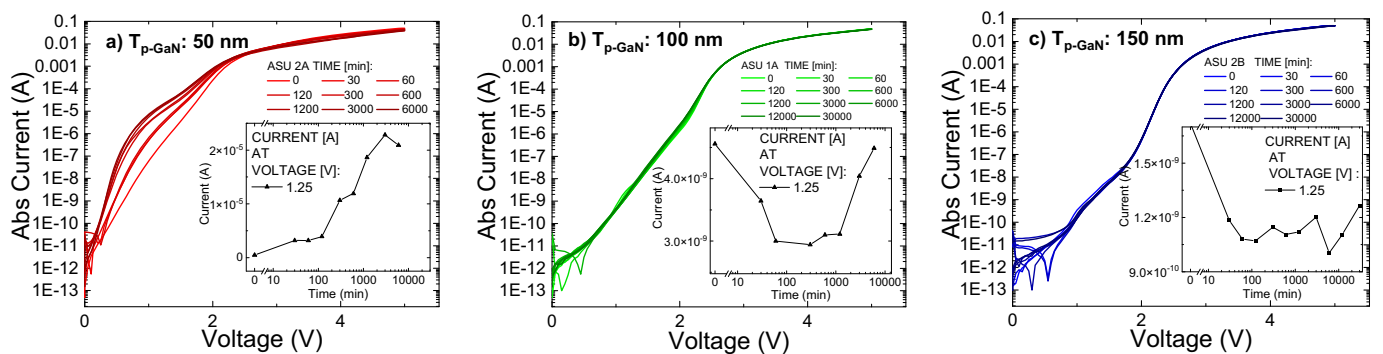


Fig. 3. Dark I-V characteristics at 35 °C after each step of the stress and current at 1.25 V (insets) for the three samples: a) 2A  $T_{p-GaN} = 50$  nm b) 1A  $T_{p-GaN} = 100$  nm c) 2B  $T_{p-GaN} = 150$  nm.

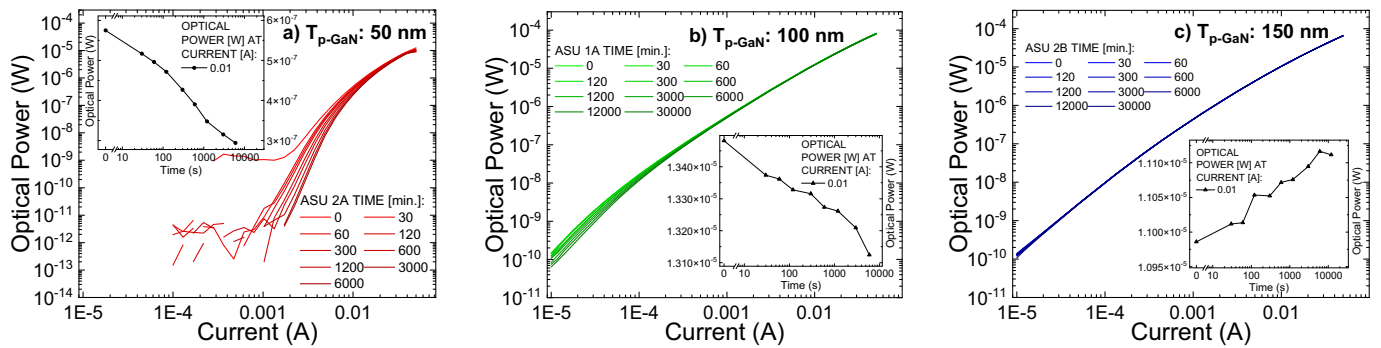


Fig. 4. Luminescence. Comparison between optical power measured at 35 °C after each step of the stress for the three samples: a) 2A  $T_{p-GaN} = 50$  nm b) 1A  $T_{p-GaN} = 100$  nm c) 2B  $T_{p-GaN} = 150$  nm. In the insets is present the optical power trend at a driving current of 0.01 A.

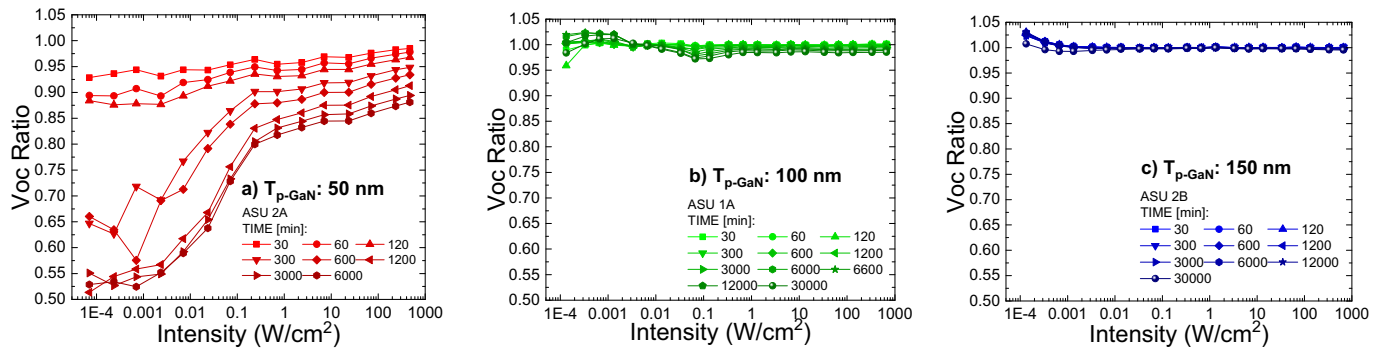


Fig. 5. Voc ratio. Comparison between the ratio of the illuminated Voc measured before the first step of the stress and the illuminated Voc measured at the end of each step stress for the three samples: a) 2A  $T_{p-GaN} = 50$  nm b) 1A  $T_{p-GaN} = 100$  nm c) 2B  $T_{p-GaN} = 150$  nm.

#### 4. Conclusion

InGaN-GaN MQWs solar cells were stressed under 405 nm monochromatic excitation at high temperature and characterized by means of dark and illuminated I-V, photocurrent and electroluminescence measurements. The constant optical power stress experiments at 175 °C carried out on devices with different p-GaN thicknesses showed a significant degradation only for the sample with the thinnest  $T_{p-GaN} = 50$  nm (namely 2A). This degradation consists in a reduction in the short-circuit current measured during the stress, in a lowering in luminescence and open-circuit voltage under illumination and in an increase in low forward leakage in dark conditions. Considering that this degradation occurs at 175 °C mainly for the sample with thinnest p-GaN, and that degradation kinetics showed a square-root dependence on time, we suggest a possible role of diffusion in degradation processes. For the other samples with a larger p-GaN, we suggest that the thicker layer reduces the amount of impurities which can reach the active region from the layers of the device (ITO,  $p^+$ -GaN and their interface), resulting in a reduced degradation during the stress. Traps levels involved in device degradation are possibly deep states, rather than shallow levels, since they impact on leakage current and on electroluminescence signal.

#### Declaration of competing interest

The authors declare that they have no known competing financial interests or personal relationships that could have appeared to influence the work reported in this paper.

#### Acknowledgments

The work at University of Padova was partly performed within project INTERNET OF THINGS: SVILUPPI METODOLOGICI,

TECNOLOGICI E APPLICATIVI, co-founded (2018-2022) by the Italian Ministry of Education, Universities and Research (MIUR) under the aegis of the “Fondo per il finanziamento dei dipartimenti universitari di eccellenza” initiative (Law 232/2016). The work at Arizona State University and Rice University was partially supported by ULTRA, an Energy Frontier Research Center (EFRC) funded by the U.S. Department of Energy, Office of Science, Basic Energy Sciences under Award # DE-SC0021230.

#### References

- [1] Best Research-Cell Efficiency Chart | Photovoltaic Research, NREL, 2022 accessed Feb. 11, <https://www.nrel.gov/pv/cell-efficiency.html>.
- [2] R. Dahal, J. Li, K. Aryal, J.Y. Lin, H.X. Jiang, InGaN/GaN multiple quantum well concentrator solar cells, *Appl. Phys. Lett.* 97 (7) (Aug. 2010), 073115, <https://doi.org/10.1063/1.3481424>.
- [3] G. Moses, X. Huang, Y. Zhao, M. Auf der Maur, E.A. Katz, J.M. Gordon, InGaN/GaN multi-quantum-well solar cells under high solar concentration and elevated temperatures for hybrid solar thermal-photovoltaic power plants, *Prog. Photovolt. Res. Appl.* 28 (11) (2020) 1167–1174, <https://doi.org/10.1002/ppp.3326>.
- [4] C. de Santi, et al., GaN-based laser wireless power transfer system, *Materials* 11 (1) (2018) 153, <https://doi.org/10.3390/MA11010153>, Jan. 2018.
- [5] Y. Zhao, et al., InGaN-based solar cells for space applications, *Midwest Symposium on Circuits and Systems 2017-August (2017)* 954–957, <https://doi.org/10.1109/MWSCAS.2017.8053083>, Sep.
- [6] D.H. Lien, et al., Harsh photovoltaics using InGaN/GaN multiple quantum well schemes, *Nano Energy* 11 (Jan. 2015) 104–109, <https://doi.org/10.1016/j.nanoen.2014.10.013>.
- [7] X. Huang, et al., Energy band engineering of InGaN/GaN multi-quantum-well solar cells via AlGaIn electron- and hole-blocking layers, *Appl. Phys. Lett.* 113 (4) (Jul. 2018), 043501, <https://doi.org/10.1063/1.5028530>.
- [8] N. Roccatto, et al., Modeling the electrical characteristics of InGaN/GaN LED structures based on experimentally-measured defect characteristics, *J. Phys. D: Appl. Phys.* 54 (42) (Aug. 2021), 425105, <https://doi.org/10.1088/1361-6463/AC16FD>.
- [9] M. Auf Der Maur, B. Galler, I. Pietzonka, M. Strassburg, H. Lugauer, A. di Carlo, Trap-assisted tunneling in InGaN/GaN single-quantum-well light-emitting diodes, *Appl. Phys. Lett.* 105 (13) (2014) Sep, <https://doi.org/10.1063/1.4896970>.

- [10] M. Mandurrino, et al., Physics-based modeling and experimental implications of trap-assisted tunneling in InGaN/GaN light-emitting diodes, *Physica Status Solidi (A) Applications and Materials Science* 212 (5) (2015) 947–953, <https://doi.org/10.1002/PSSA.201431743>, May.
- [11] K. Orita, et al., Analysis of diffusion-related gradual degradation of InGaN-based laser diodes, *IEEE J. Quantum Electron.* 48 (9) (2012) 1169–1176, <https://doi.org/10.1109/JQE.2012.2203795>.
- [12] H. Xing, et al., Memory effect and redistribution of Mg into sequentially regrown GaN layer by metalorganic chemical vapor deposition, *Japanese Journal of Applied Physics, Part 1: Regular Papers and Short Notes and Review Papers* 42 (1) (Jan. 2003) 50–53, <https://doi.org/10.1143/JJAP.42.50/XML>.
- [13] D.W. Kim, Y.J. Sung, J.W. Park, G.Y. Yeom, A study of transparent indium tin oxide (ITO) contact to p-GaN, *Thin Solid Films* 398–399 (Nov. 2001) 87–92, [https://doi.org/10.1016/S0040-6090\(01\)01368-2](https://doi.org/10.1016/S0040-6090(01)01368-2).
- [14] S.J. Pearton, H. Cho, J.R. LaRoche, F. Ren, R.G. Wilson, J.W. Lee, Oxygen diffusion into SiO<sub>2</sub>-capped GaN during annealing, *Appl. Phys. Lett.* 75 (19) (Nov. 1999) 2939, <https://doi.org/10.1063/1.125194>.
- [15] A. Caria, M. Nicoletto, C. De Santi, M. Buffolo, Xuanqi Huang, Houqiang Fu, Hong Chen, Yuji Zhao, G. Meneghesso, E. Zanoni, M. Meneghini, Quantum efficiency of InGaN-GaN multi-quantum well solar cells: Experimental characterization and modeling, *J. Appl. Phys.* 131 (2022), <https://doi.org/10.1063/5.0076833>. In press.
- [16] M. Nicoletto, et al., Characterization and Modeling of Quantum Efficiency InGaN-GaN Multi-Quantum Well (MQW) solar cells, in: Presented at the 45th WOCSDICE/EXMATEC Conference, Ponta Delgada, Portugal, 3-6 May, 2022, pp. 25–26.